

Article

Atomic Layer Deposition of Lithium Fluoride Optical Coatings for the Ultraviolet

John Hennessy *  and Shouleh Nikzad

Jet Propulsion Laboratory, California Institute of Technology, 4800 Oak Grove Dr, Pasadena, CA 91109, USA; shouleh.nikzad@jpl.nasa.gov

* Correspondence: john.j.hennessy@jpl.nasa.gov

Received: 4 April 2018; Accepted: 28 April 2018; Published: 4 May 2018



Abstract: Lithium fluoride is an important material for ultraviolet optical systems, possessing among the largest optical bandgaps of dielectric materials. We report on the development of an atomic layer deposition (ALD) process for lithium fluoride that is capable of depositing thin films in a self-limiting manner, with an approximate deposition rate of approximately 0.15 Å per ALD cycle at a substrate temperature of 150 °C. Films are characterized by spectroscopic ellipsometry, atomic force microscopy, X-ray photoelectron spectroscopy, and far ultraviolet reflectometry. For substrate temperatures of 150 °C and greater, films showed significant microroughness with a correlated reduction in effective refractive index. This behavior was mitigated by a reduction in substrate temperature to as low as 100 °C. Films deposited on silicon substrates were subjected to long-term storage testing to evaluate the environmental sensitivity of the deposited layers. Protected aluminum mirrors were also fabricated with ALD LiF overcoats, yielding a reflectance of 84% at a wavelength of 125 nm. The performance relative to state-of-the-art LiF thin films deposited by physical vapor deposition methods is discussed, along with the prospects for future optimization.

Keywords: atomic layer deposition; lithium fluoride; ultraviolet; thin film; atomic layer etching; mirror

1. Introduction

The use of lithium fluoride (LiF) as an ultraviolet optical coating material is motivated by its large optical bandgap, exceeding that of other metal fluoride materials used for this application such as magnesium fluoride (MgF₂) and aluminum fluoride (AlF₃). Thin films of LiF have also seen utility as components in cathode coating layers of Li-ion batteries [1], as thermoluminescent detector layers for X-ray and extreme ultraviolet sensor applications [2], and for electron injection layers in some light-emitting diodes or photovoltaics [3,4].

The transparency of LiF into the far ultraviolet (FUV, $\lambda = 90\text{--}200$ nm) has also led to its use as a protective coating for aluminum mirrors [5]. Aluminum possesses the highest natural reflectance in the FUV, but its natural oxide is strongly absorbing at these wavelengths. Therefore, the production of Al mirrors typically involves immediate encapsulation of the metal layer with a protective transparent coating to preserve performance at the shortest wavelength possible. In this case, loss in the protective coating dominates the short wavelength reflectance of the mirror; MgF₂/Al can typically provide meaningful reflectance ($R > 50\%$) down to ~ 115 nm, AlF₃/Al down to ~ 110 nm, and LiF/Al down to ~ 100 nm. This has motivated the use of LiF/Al mirrors on optical telescope systems in space applications when the desired scientific observations require this FUV throughput [6,7].

Thin films of LiF and other metal fluorides are commonly deposited by physical vapor deposition (PVD) methods, such as evaporation [5,8–10] or sputtering [11]. Recently, several processes for the atomic layer deposition (ALD) of LiF have also been reported. The use of ALD is attractive for protected mirror applications in the context of improving the reflectance uniformity of large diameter

optical systems. For a metallic film with a uniform reflectance, the transparent overcoat can degrade the uniformity of response via thin film interference effects; this can become an important source of wavefront error in large aperture systems. Future space telescope mission concepts are considering the use of LiF-protected mirrors at much larger apertures, and with many more segments, than previously implemented [12]. The self-limiting nature of ALD yields a thin film deposition process with inherent uniformity and scalability that may be able to meet the reflectance uniformity and repeatability needs of these future missions.

Mantymaki et al. have reported LiF ALD via alternating exposure to Li(thd) and two alternate routes that include exposure to TiF_4 [13,14]. Lee et al. has described deposition via lithium bis(trimethylsilyl)amide (LiHMDS) and hydrogen fluoride (HF) sourced from a solution of HF-pyridine [15]. Alternate metal fluorides have also been demonstrated via an oxide chemistry route that involves fluorination by hexafluoroacetylacetonate compounds [16]. Previous work in our lab has explored the ALD of MgF_2 and AlF_3 for the same UV applications, utilizing anhydrous HF as the fluorine-containing precursor [17,18]. We have also produced preliminary FUV mirror results for Al protected with these materials [19,20] and multilayer filter stacks comprised of Al and metal fluorides for FUV detector-integrated filters [21]. In this work, we expand this anhydrous HF approach to the deposition of LiF and assess the morphology, composition, and optical properties of the resulting thin films. Measurements of FUV reflectance are demonstrated for LiF deposited on Si substrates as well as Al layers to evaluate the potential of this material for FUV mirror applications.

2. Atomic Layer Deposition Properties

Films were deposited by alternating exposure to LiHMDS and anhydrous HF. The self-limiting properties of the process were explored by investigating the influence of precursor delivery time and purge time on the resulting film thickness. Each ALD cycle involved a single LiHMDS exposure, followed by a purging of the vacuum chamber with inert gas, and then HF exposure along with an additional purge. Initial testing indicated a maximum deposition rate at a substrate temperature of 150 °C; therefore, the majority of the process optimization was performed at this temperature. As indicated in Figure 1a, pulse times of 3 s for LiHMDS were sufficient to result in a saturated deposition rate per ALD cycle. There was less overall dependence on the delivered HF dose; no apparent reduction in growth per cycle (GPC) was observed down to the minimum possible valve pulse time of 15 ms. Purge times of 10 s and 45 s were used following LiHMDS and HF exposures, respectively. For longer purge times, little variation in deposition rate was observed.

The linearity of film thickness versus number of ALD cycles was observed to fall off for many cycles, as shown in Figure 1b. This has been a result of an increase in effective surface area, as the surface roughness evolved as a function of film thickness. The morphology of the resulting films was investigated by atomic force microscopy (AFM). As indicated in Figure 2, films deposited on silicon substrates showed significant apparent crystallinity and a correspondingly large surface roughness that increased with film thickness. The degree of crystallinity, relative grain size, and values of surface roughness appeared roughly consistent with other reports of LiF deposition, whether by ALD methods [13] or PVD methods [10,22]. For comparison, MgF_2 films deposited in the same ALD system possessed crystallinity with much smaller grain size and showed a root-mean-square (rms) surface roughness over the same spatial scale of 0.8 nm for 25 nm thick films deposited at 150 °C [17]. Thin films of AlF_3 in the same system, which were amorphous as-deposited, showed a roughness of only 0.3 nm for 25 nm thick films at 150 °C [18].

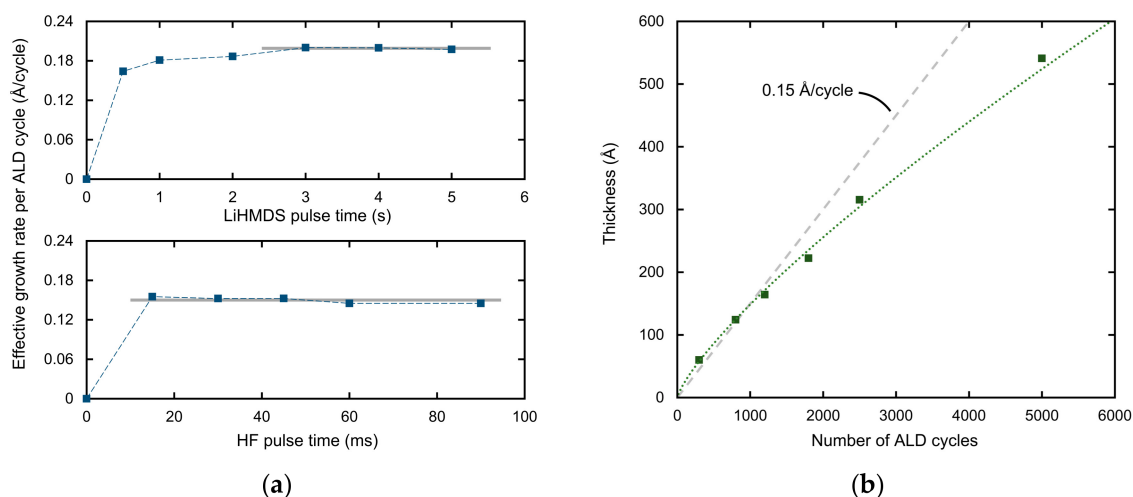


Figure 1. (a) The dependence of ALD deposition rate on LiHMDS and HF exposure time. The LiHMDS experiments were performed for 300 ALD cycles for each data point; the HF experiments used 600 ALD cycles; (b) The measured film thickness versus number of ALD cycles, which indicated a degradation in linearity for films deposited at a substrate temperature of 150 °C.

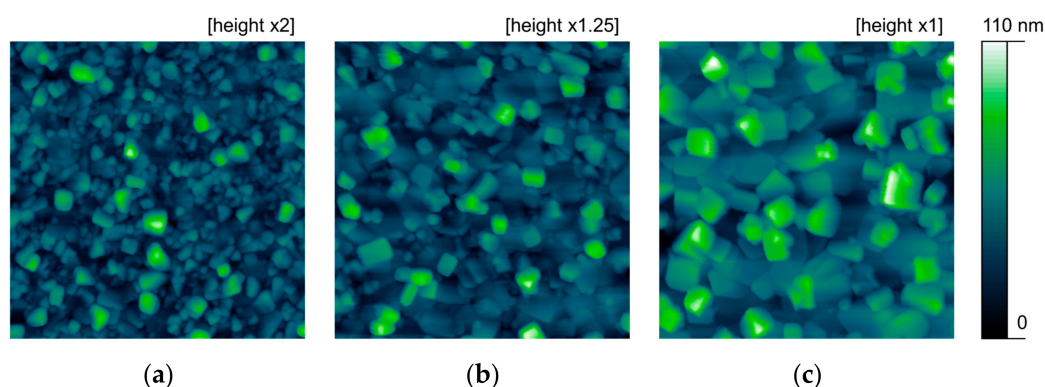


Figure 2. Representative AFM images of LiF films deposited on Si substrates at 150 °C over a $1 \times 1 \mu\text{m}^2$ area for a varying number of ALD cycles, with the corresponding effective thickness (t), and the rms roughness (S_q) averaged over five spots on each sample: (a) 1300 cycles, $t = 19 \text{ nm}$, $S_q = 6.8 \pm 0.3 \text{ nm}$; (b) 2500 cycles, $t = 33 \text{ nm}$, $S_q = 11.5 \pm 0.3 \text{ nm}$; (c) 5000 cycles, $t = 56 \text{ nm}$, $S_q = 18.7 \pm 1.7 \text{ nm}$.

3. Lithium Fluoride Film Properties

Film thickness as described in the previous section was characterized by phase-modulated spectroscopic ellipsometry. The samples receiving 1300, 1800, 2500, and 5000 cycles of deposition were fit simultaneously over the wavelength range of 350–885 nm at measured incident angles of 50 and 70 degrees. A transparent Cauchy model was used to estimate the refractive index taking the form:

$$n(\lambda) = A + B \times 10^4 / \lambda^2, \quad (1)$$

with λ expressed in nanometers. The best fit yielded values of $A = 1.27$ and $B = 0.19 (\pm 0.04)$ for this set of thin films deposited at 150 °C. This value of refractive index was lower than typically reported values for either single crystal or thin film LiF, which are typically in the range of $n = 1.37$ – 1.40 at visible wavelengths [23,24]. These values were used to calculate the film thicknesses which appear in Figure 1. The reduced value of refractive index implies a reduced packing density, or the influence of significant roughness effects, or a combination of the two. This hypothesis was queried by evaluating the trend in optical fitting at shorter wavelengths for each film thickness individually. Extending the fitting range into the near ultraviolet (NUV, $\lambda = 200$ – 400 nm) covering 190–885 nm was observed to degrade the

goodness-of-fit for each sample. To constrain the optical model and reduce cross-correlation between parameters, each set of ellipsometric data was fit simultaneously with measurements of near-normal reflectance, and the B parameter was fixed to the previous value of 0.19. The trend for increasing film thickness is summarized in Table 1, which shows an increasing value of χ^2 for increasing values of film thickness.

Table 1. The results of ellipsometric and reflectance fitting over the wavelength range of 190–885 nm for LiF films deposited with an increasing number of ALD cycles and fit to a single parameter Cauchy model.

No. of ALD Cycles	Index Param., A	Eff. Thickness (nm)	χ^2
1300	1.25	19	0.14
1800	1.24	22	0.35
2500	1.28	31	1.79
5000	1.28	50	27.5
5000 *	1.40	36/61	3.60

* Fit with an additional surface layer to approximate roughness effects.

Increasing loss via absorption at short wavelengths could be responsible for such an increase, but index models incorporating such a loss resulted in convergence to unphysical index relations. An attempt to account for the increased surface roughness was made by including an additional layer in the optical model, formed of a mixture of free space and the LiF constants being fit. The optical properties of this mixture were calculated using a Bruggeman effective medium model. As noted in Table 1, the goodness-of-fit was notably improved in the case where this roughness layer was added. This procedure resulted an effective index of the LiF layer of 1.40, which is more in accordance with expected values. The results of this improved fitting procedure are shown in Figure 3, with the measured ellipsometric parameters and near-normal reflectance in comparison to model predictions with and without the added roughness layer. The ellipsometric parameters, I_S and I_C , were again fit at both 50 and 70 degree angle of incidence; for clarity, only the 70 degree data is plotted in Figure 3. Notably, there remained some discrepancy in the optical model for this film thickness, particularly at shorter wavelengths. This may have been the result of additional losses from scatter or absorption that were not accounted for here.

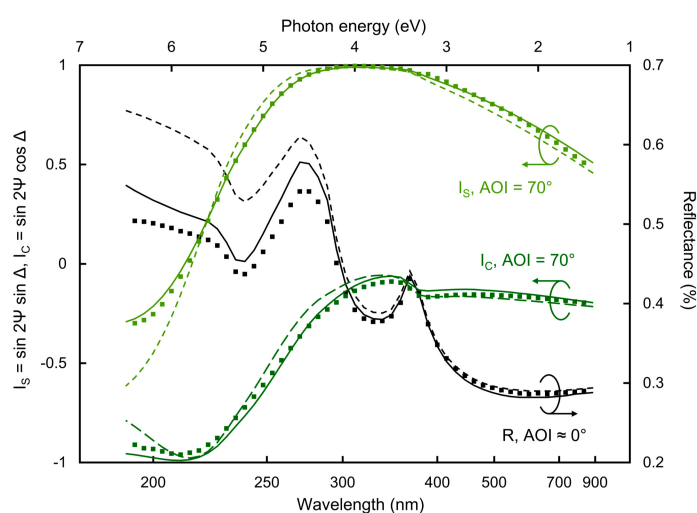


Figure 3. The measured ellipsometric parameters, I_S and I_C , at an angle of incidence of 70° , and the measured near-normal reflectance for 5000 cycles of LiF deposition at a substrate temperature of 150°C (symbols). The best simultaneous fit for a single optical layer (dashed line) is shown, along with the best fit for an additional layer to approximate surface roughness effects (solid line).

At reduced substrate temperature, film roughness was improved. As an example, a 19 nm thick film deposited at 100 °C showed a rms roughness of 3.2 ± 0.1 nm versus 6.8 ± 0.3 nm for films of the same thickness deposited at 150 °C (see Figure 2). Ellipsometric fitting yielded index parameters for the same Cauchy model described above of $A = 1.36 (\pm 0.01)$ and $B = 0.20 (\pm 0.04)$. This represents a refractive index that is in better agreement with reference values, suggesting that the film density was improved at this lower substrate temperature. The deposition rate was approximately 0.1 Å per cycle at 100 °C. At higher substrate temperatures the roughness and measured optical properties of the resulting films were similar to those deposited at 150 °C. Notably, the same detailed optical fitting procedure was not performed for films deposited at other substrate temperatures. The ALD growth per cycle was also observed to decline at elevated temperatures, reaching only 0.1 Å per cycle at 250 °C. Temperatures higher than 250 °C were not explored, as this was already above the expected decomposition temperature of LiHMDS [25].

Film composition was studied by X-ray photoelectron spectroscopy (XPS). Films approximately 3 nm-thick deposited on Si substrates were investigated to minimize charging effects. The measured binding energies were referenced to place the adventitious C 1s level at 284.8 eV. Figure 4 shows the resulting high resolution Li 1s and F 1s regions; the peak energy agreed well with reported binding energies for LiF [26]. Using these components, estimates of film stoichiometry were made by comparing the relative area of each peak and adjusting by relative system sensitivity factors. This yielded a Li:F ratio of $1.1 (\pm 0.1)$ to 1, indicating the films were approximately stoichiometric as deposited. Residual carbon and oxygen impurities were not studied as part of this experiment.

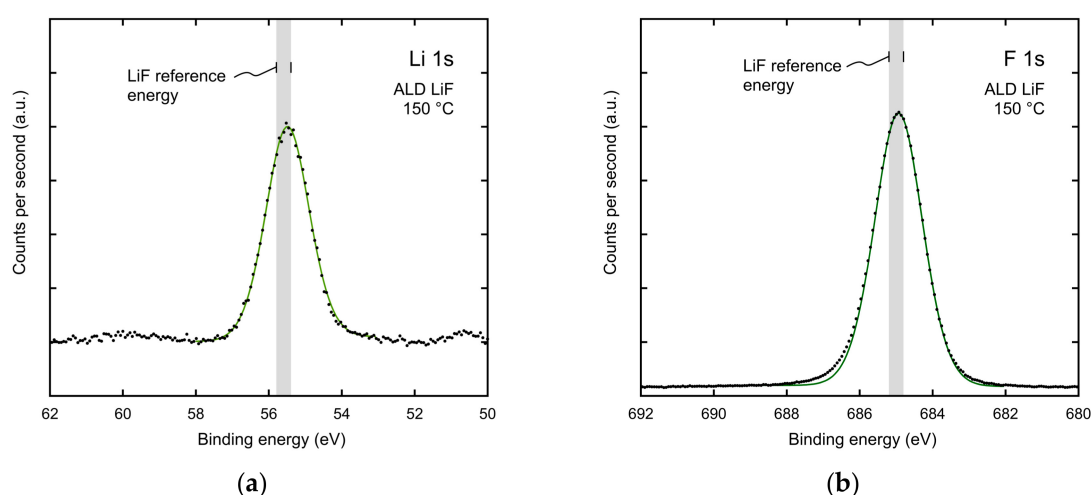


Figure 4. High-resolution XPS spectra (symbols) and the background-adjusted best-fit (solid line) of the (a) Li 1s level, and (b) the F 1s level, for a 3 nm ALD LiF thin film deposited on Si at a substrate temperature of 150 °C. Shaded regions highlight expected binding energies for LiF from reference spectra [26].

4. Far Ultraviolet Characterization

One of the primary interests in LiF is the extension of the performance of optical and protective coatings to shorter wavelengths in the FUV. The wavelength of strong absorption is typically shorter than other metal fluoride materials; however, other loss mechanisms tend to reduce the performance of LiF at longer wavelengths, particularly for thin film applications. This is often attributed to the environmental sensitivity of LiF and its possible reactivity with residual water vapor in the air [8,27]. In protected Al mirror systems, a degradation of reflectance for long duration storage is generally observed, even in nominally dry conditions [8]. This has led to the development of multilayer protective coatings where thin layers of MgF₂ or AlF₃ may be inserted before and/or after the encapsulation of the Al layer with LiF [10,28,29]. The evaporation of LiF at elevated temperatures has been shown to

increase the as-deposited reflectance of protected Al mirrors [9] and reduce the amount of reflectance loss experienced during long-term storage [8].

To probe the environmental sensitivity of our deposited LiF layers, we evaluated the FUV reflectance of Si substrates coated with 30 nm of LiF deposited at 150 °C over a period of several months. Silicon substrates were chosen in this case to differentiate the effects of LiF aging from the possible degradation or oxidation of an Al layer in a protected mirror system. Figure 5a shows the change in measured reflectance for a sample stored in ambient cleanroom conditions (regulated to 40% relative humidity, 22 °C) over a total period of 16 weeks. Some loss in reflectance was observed which was similar to the relative loss experienced in recent high-temperature PVD mirror experiments [28]. Figure 1b shows that this loss appeared to saturate over time. Intermediate storage in dry nitrogen of samples deposited during the same LiF run appeared to slow the rate of reflectance loss but did not completely eliminate it.

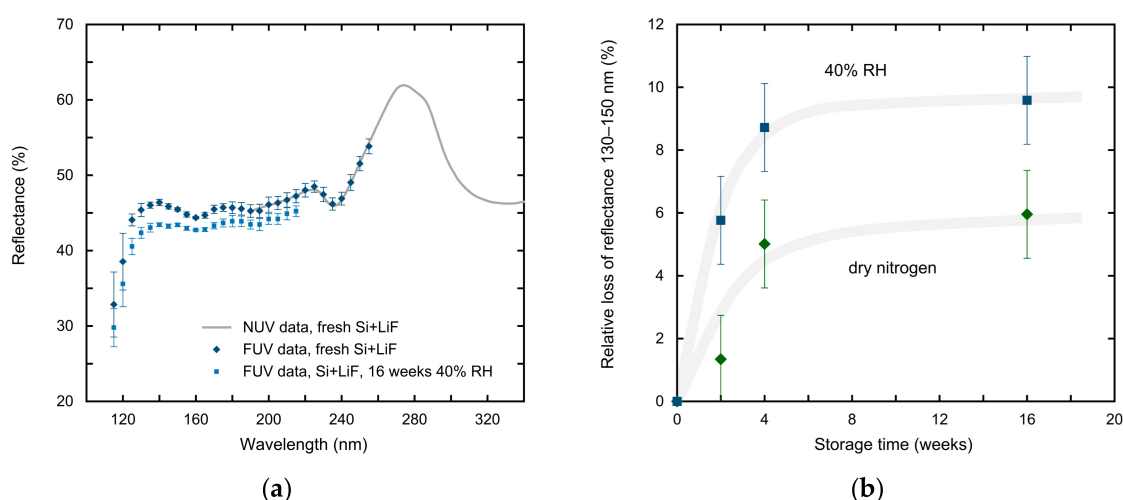


Figure 5. (a) The measured FUV and NUV reflectance of 30 nm of LiF deposited on silicon measured immediately following deposition and after 16 weeks of storage at 40% RH at room temperature; (b) The relative change in reflectance average over 130–150 nm for samples in 40% RH versus samples stored in dry nitrogen.

Aluminum mirrors protected with ALD LiF were also investigated in a separate experiment. The deposition of Al was performed by electron beam evaporation onto 50 mm Si substrates and transferred ex situ to the ALD chamber. Samples were allowed to oxidize to completion over the course of several days. The surface oxide layer was then removed with an atomic layer etching (ALE) procedure that has been described elsewhere [30]. Removal of the native oxide is critical for achieving high reflectance at FUV wavelengths. The ability to perform a low temperature selective etch process inside the ALD chamber enables the combination of PVD Al with ALD fluoride overcoats without the need for complex dual-use systems or vacuum-transfer methods. Recent reports have demonstrated ALD methods for Al thin films with good electrical properties [31]. This may enable an all-ALD process capable of depositing both the metal layer and protective overcoat without a vacuum break. However, the optical quality of Al thin films deposited by ALD or other chemical vapor deposition methods has not yet been demonstrably comparable in performance to PVD methods, particularly in the UV.

The ALE process was initiated at a substrate temperature of 210 °C; at higher temperatures the oxide etch rate was increased, but the selectivity with the underlying Al was degraded. At lower temperatures, the etch rate decreased, and the process could also become poisoned by unintentional deposition of AlF_3 . Following the ALE procedure, Al encapsulation was performed by the LiF ALD procedure, described in previous sections, as the substrate temperature was reduced to 100 °C. The reduced temperature relative to the majority of the optical characterization described previously

was chosen for the possible benefits of reduced surface roughness; it also allowed for more rapid subsequent encapsulation of the deposited LiF layer with thin AlF_3 . Previous experiments have indicated a significant chemical interaction between the precursors required for AlF_3 deposition and LiF at temperatures significantly greater than $100\text{ }^\circ\text{C}$ [30].

As indicated in Figure 6, two samples were created with the same LiF process to a target thickness of 18 nm. One was removed as the table temperature was further reduced to $75\text{ }^\circ\text{C}$ to perform approximately 2 nm of ALD AlF_3 deposition. The performance of these mirror prototypes is a good indicator of the optical quality of these ALD layers. The FUV reflectance of the AlF_3 -protected sample slightly exceeded the unprotected LiF sample; however, it is not clear if this can be attributed to a difference in optical thickness or a degradation experienced by the unprotected samples during the brief period it was exposed to the ambient environment prior to loading into the vacuum characterization system (approximately 10 min duration). Additional environmental studies, similar to the evaluation shown in Figure 5, are required to accurately assess the efficacy of the AlF_3 encapsulation.

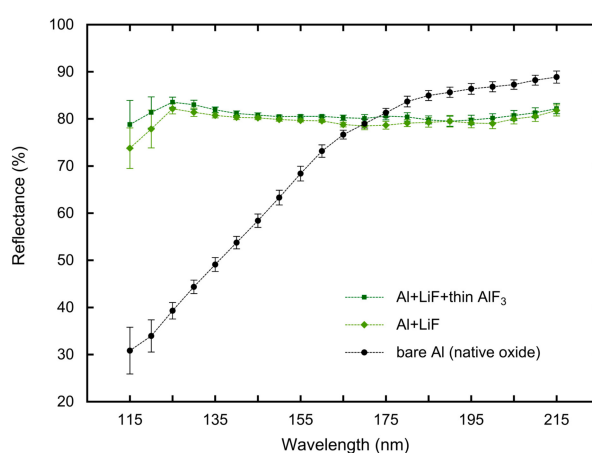


Figure 6. The measured FUV reflectance of Al mirrors protected with 18 nm ALD LiF films deposited at $100\text{ }^\circ\text{C}$. One sample was coated with an additional 2 nm of ALD AlF_3 as an initial test of encapsulation strategies to limit environmental sensitivity of the underlying LiF.

The peak FUV reflectance of 84% at 125 nm exceeded historical examples of evaporated LiF-protected Al mirrors, for example, telescope mirrors fabricated for the Far Ultraviolet Spectroscopic Explorer mission only reached a reflectance of 60–65% in this wavelength range [6]. For a notional three-mirror telescope system including primary, secondary, and fold optics, this performance improvement with ALD LiF would more than double the overall throughput relative to these legacy coatings. The ALD mirrors are comparable to more recent PVD examples that utilize elevated substrate temperatures and can reach 80–90% reflectance in the FUV [9,10]. Although there is significant technical interest in the performance of LiF-protected Al mirrors at wavelengths below 115 nm, this exceeds our current measurement capabilities.

5. Conclusions and Future Directions

In this work, we have demonstrated that thin films of LiF can be deposited in a self-limiting manner over a temperature range of $100\text{--}250\text{ }^\circ\text{C}$, with potential applications related to FUV optical coatings. The films possessed significant crystallinity, which resulted in moderate surface roughness compared to typical dielectric materials deposited by ALD. Measurements of the FUV reflectance of LiF deposited on Si substrates indicated an aging effect that was similar to previous studies on films deposited by PVD methods. Nevertheless, protected Al mirrors can be fabricated with LiF overcoats and yield reflectance that is comparable to the best-reported examples of LiF-protected Al mirrors fabricated by PVD methods. The fabrication of these mirrors was facilitated by an ALE process that

allowed for the combination of evaporated Al and ALD protective coatings without the requirement of a shared-vacuum system.

In future work, we will explore larger substrate areas and shaped optics to evaluate the benefits of the ALD method with respect to reflectance uniformity. We will also expose these mirror systems to long-duration storage testing to evaluate their environmental sensitivity and study compositional changes as a function of time and environment. This sensitivity may have a dependence on LiF deposition conditions such as substrate temperature, which has been shown to be important for PVD films. The roughness and environmental sensitivity can potentially be addressed through consideration of nanolaminates of LiF and other fluoride materials. Because the ALD method can yield film growth with monolayer or sub-monolayer control, it is possible to engineer the composition of the FUV optical coating with the inclusion of subcycles of MgF_2 or AlF_3 . In this way, there may be tunability with respect to exchanging short-wavelength performance for stability. This approach has been successful in other ALD systems, such as the inclusion of alumina cycles during the ALD of hafnia thin films to control morphology [32]. Future work will also seek to characterize these mirror systems at wavelengths shorter than 115 nm to assess their suitability for future FUV astrophysics instruments.

6. Materials and Methods

Thin film depositions of LiF were performed in a showerhead-style reactor (Oxford OpAL, Abingdon, UK) using alternating pulses of LiHMDS (SAFC, 97%, Haverhill, MA, USA) and anhydrous HF (Matheson Tri-Gas, 4N5 purity, Newark, CA, USA). LiHMDS was held in a stainless steel cylinder at 70 °C and bubbled through with a carrier gas during processing. The HF was stored at room temperature and delivered through a single stage regulator and needle valve and then pulsed into the reaction chamber with conventional high-speed diaphragm valves. ALD experiments were performed using Ar (Matheson Tri-Gas, 6N purity, Newark, CA, USA) as the purge and carrier gas; each were delivered through a mass flow controller at 70 sccm. Aluminum fluoride encapsulation layers were deposited via trimethylaluminum (SAFC, 97%, Haverhill, MA, USA) and anhydrous HF. The ALE process used to etch native Al oxide also used cyclic exposure to trimethylaluminum and HF but at higher substrate temperatures.

Film composition was studied by XPS on a Surface Science Instruments M-Probe ESCA (Mountain View, CA, USA) equipped with a 1486.6 eV Al $K\alpha$ monochromatic X-ray source. The vacuum chamber was operated at a pressure of less than 8×10^{-9} Torr, and no surface sputtering or active charge compensation was performed in these experiments. Surface roughness was characterized by AFM on a Park Systems NX20 (Suwon, Korea) with a characterization area of $1 \times 1 \mu\text{m}$. All samples were measured in non-contact mode; final images were flattened to remove global tilt but with no additional filtering. Reported values of rms roughness were averaged over five different spots on each sample.

For mirror experiments, Al films were deposited by electron beam evaporation onto Si substrates. The system was pumped until a base pressure of less than 5×10^{-8} Torr was obtained. Aluminum was deposited to a target thickness of 55 nm at a deposition rate of 15 nm/s. This high rate ensured improved film composition and morphology, which can dramatically affect the FUV reflectance of Al films [20]. The bare Al samples evaporated under these conditions exhibited an rms roughness of 0.58 ± 0.03 nm, as characterized by the AFM conditions described above. The film thickness and the evaporation rate were monitored during deposition by quartz crystal microbalance and verified after completion by resistivity measurements.

Lithium fluoride film thickness and refractive index were characterized by spectroscopic phase-modulated ellipsometry on a Horiba Uvisel 2 (Longjumeau, France). Measurements of near-normal incidence NUV reflectance were performed relative to a bare Si wafer using a Filmetrics F20UV spectrometer (San Diego, CA, USA). The far ultraviolet reflectance of LiF deposited on both Si and Al was measured on an Acton VM 502 vacuum monochromator (Acton, MA, USA). The system was operated at a base pressure of less than 1×10^{-4} Torr, and samples were illuminated by a deuterium lamp through a MgF_2 window. The FUV measurements were collected in 1 Å intervals by

continuously stepping the grating position and then binning the raw data in 5 nm intervals after a linear correction for wavelength errors.

Author Contributions: J.H. and S.N. conceived and designed the experiments; J.H. performed the experiments, analyzed the data, and wrote the paper.

Acknowledgments: This research has been performed in part at the Jet Propulsion Laboratory, California Institute of Technology, under a contract with the National Aeronautics and Space Administration.

Conflicts of Interest: The authors declare no conflict of interest.

References

1. Xie, J.; Sendek, A.D.; Cubuk, E.D.; Zhang, X.; Lu, Z.; Gong, Y.; Wu, T.; Shi, F.; Liu, W.; Reed, E.J.; et al. Atomic layer deposition of stable LiAlF₄ lithium ion conductive interfacial layer for stable cathode cycling. *ACS Nano* **2017**, *11*, 7019–7027. [[CrossRef](#)] [[PubMed](#)]
2. Montekali, R.M.; Bonfigli, F.; Piccinini, M.; Nichelatti, E.; Vincenti, M.A. Photoluminescence of colour centres in lithium fluoride thin films: From solid-state miniaturised light sources to novel radiation imaging detectors. *J. Lumin.* **2016**, *170*, 761–769. [[CrossRef](#)]
3. Hung, L.S.; Tang, C.W.; Mason, M.G. Enhanced electron injection in organic electroluminescence devices using an Al/LiF electrode. *Appl. Phys. Lett.* **1997**, *70*, 152–154. [[CrossRef](#)]
4. Bullock, J.; Zheng, P.; Jeangros, Q.; Tosun, M.; Hettick, M.; Sutter-Fella, C.M.; Wan, Y.; Allen, T.; Yan, D.; Macdonald, D.; et al. Lithium Fluoride Based Electron Contacts for High Efficiency n-Type Crystalline Silicon Solar Cells. *Adv. Energy Mater.* **2016**, *6*, 1600241. [[CrossRef](#)]
5. Hunter, W.R.; Osantowski, J.F.; Hass, G. Reflectance of aluminum overcoated with MgF₂ and LiF in the wavelength region from 1600 Å to 300 Å at various angles of incidence. *Appl. Opt.* **1971**, *10*, 540–544. [[CrossRef](#)] [[PubMed](#)]
6. Ohl, R.G.; Barkhouser, R.H.; Conard, S.J.; Friedman, S.D.; Hampton, J.; Moos, H.W.; Nikulla, P.; Oliveira, C.M.; Saha, T.T. Performance of the Far Ultraviolet Spectroscopic Explorer mirror assemblies. *Proc. SPIE* **2000**, *4139*, 137–149. [[CrossRef](#)]
7. France, K.; Hoadley, K.; Fleming, B.T.; Kane, R.; Nell, N.; Beasley, M.; Green, J.C. The SLICE, CHESS, and SISTINE ultraviolet spectrographs: Rocket-borne instrumentation supporting future astrophysics missions. *J. Astron. Instrum.* **2016**, *5*, 1640001. [[CrossRef](#)]
8. Hutcheson, E.T.; Hass, G.; Cox, J.T. Effect of deposition rate and substrate temperature on the vacuum ultraviolet reflectance of MgF₂- and LiF-overcoated aluminum mirrors. *Appl. Opt.* **1972**, *11*, 2245–2248. [[CrossRef](#)] [[PubMed](#)]
9. Quijada, M.A.; Del Hoyo, J.; Rice, S. Enhanced far-ultraviolet reflectance of MgF₂ and LiF over-coated Al mirrors. *Proc. SPIE* **2014**, *9144*, 91444G. [[CrossRef](#)]
10. Wilbrandt, S.; Stenzel, O.; Nakamura, H.; Wulff-Molder, D.; Duparré, A.; Kaiser, N. Protected and enhanced aluminum mirrors for the VUV. *Appl. Opt.* **2014**, *53*, A125–A130. [[CrossRef](#)] [[PubMed](#)]
11. Thompson, G.B.; Allred, D.D. Reactive gas magnetron sputtering of lithium hydride and lithium fluoride thin films. *J. X-Ray Sci. Technol.* **1997**, *7*, 159–170. [[CrossRef](#)]
12. Bolcar, M.R. The Large UV/Optical/Infrared Surveyor (LUVOIR): Decadal Mission concept technology development overview. *Proc. SPIE* **2017**, *10398*, 103980A. [[CrossRef](#)]
13. Mäntymäki, M.; Hämäläinen, J.; Puukilainen, E.; Sajavaara, T.; Ritala, M.; Leskelä, M. Atomic layer deposition of LiF thin films from Lithd, Mg(thd)₂, and TiF₄ precursors. *Chem. Mater.* **2013**, *25*, 1656–1663. [[CrossRef](#)]
14. Mäntymäki, M.; Hämäläinen, J.; Puukilainen, E.; Munnik, F.; Ritala, M.; Leskelä, M. Atomic layer deposition of LiF thin films from Lithd and TiF₄ precursors. *Chem. Vap. Depos.* **2013**, *19*, 111–116. [[CrossRef](#)]
15. Lee, Y.; Sun, H.; Young, M.J.; George, S.M. Atomic layer deposition of metal fluorides using HF–pyridine as the fluorine precursor. *Chem. Mater.* **2016**, *28*, 2022–2032. [[CrossRef](#)]
16. Putkonen, M.; Szeghalmi, A.; Pippel, E.; Knez, M. Atomic layer deposition of metal fluorides through oxide chemistry. *J. Mater. Chem.* **2011**, *21*, 14461–14465. [[CrossRef](#)]
17. Hennessy, J.; Jewell, A.D.; Greer, F.; Lee, M.C.; Nikzad, S. Atomic layer deposition of magnesium fluoride via bis(ethylcyclopentadienyl)magnesium and anhydrous hydrogen fluoride. *J. Vac. Sci. Technol. A* **2015**, *33*, 01A125. [[CrossRef](#)]

18. Hennessy, J.; Jewell, A.D.; Balasubramanian, K.; Nikzad, S. Ultraviolet optical properties of aluminum fluoride thin films deposited by atomic layer deposition. *J. Vac. Sci. Technol. A* **2016**, *34*, 01A120. [[CrossRef](#)]
19. Moore, C.S.; Hennessy, J.; Jewell, A.D.; Nikzad, S.; France, K. Recent developments and results of new ultraviolet reflective mirror coatings. *Proc. SPIE* **2014**, *9144*, 91444H. [[CrossRef](#)]
20. Hennessy, J.; Balasubramanian, K.; Moore, C.S.; Jewell, A.D.; Nikzad, S.; France, K.; Quijada, M. Performance and prospects of far ultraviolet aluminum mirrors protected by atomic layer deposition. *J. Astron. Telesc. Instrum. Syst.* **2016**, *2*, 041206. [[CrossRef](#)]
21. Nikzad, S.; Jewell, A.D.; Hoenk, M.E.; Jones, T.J.; Hennessy, J.; Goodsall, T.M.; Carver, A.G.; Shapiro, C.; Cheng, S.R.; Hamden, E.T.; et al. High-efficiency UV/optical/NIR detectors for large aperture telescopes and UV explorer missions: Development of and field observations with delta-doped arrays. *J. Astron. Telesc. Instrum. Syst.* **2017**, *3*, 036002. [[CrossRef](#)]
22. Kim, H.; King, A.H. Grain growth and texture development in lithium fluoride thin films. *J. Mater. Res.* **2008**, *23*, 452–462. [[CrossRef](#)]
23. Roessler, D.M.; Walker, W.C. Optical constants of magnesium oxide and lithium fluoride in the far ultraviolet. *J. Opt. Soc. Am.* **1967**, *57*, 835–836. [[CrossRef](#)]
24. Cox, J.T.; Hass, G.; Waylonis, J.E. Further studies on LiF-overcoated aluminum mirrors with highest reflectance in the vacuum ultraviolet. *Appl. Opt.* **1968**, *7*, 1535–1540. [[CrossRef](#)] [[PubMed](#)]
25. Hämäläinen, J.; Holopainen, J.; Munnik, F.; Hatanpää, T.; Heikkilä, M.; Ritala, M.; Leskelä, M. Lithium phosphate thin films grown by atomic layer deposition. *J. Electrochem. Soc.* **2012**, *159*, A259–A263. [[CrossRef](#)]
26. Moulder, J.F.; Stickle, W.F.; Sobol, P.E.; Bomben, K.D. *Handbook of X-ray Photoelectron Spectroscopy*; Chastain, J., Ed.; Perkin-Elmer Corporation: Eden Prairie, MN, USA, 1992; pp. 34–35, ISBN 0962702625.
27. Oliveira, C.M.; Retherford, K.; Conard, S.J.; Barkhouser, R.H.; Friedman, S.D. Aging studies of LiF-coated optics for use in the far ultraviolet. *Proc. SPIE* **1999**, *3765*, 52–61. [[CrossRef](#)]
28. Fleming, B.; Quijada, M.; Hennessy, J.; Egan, A.; Del Hoyo, J.; Hicks, B.A.; Wiley, J.; Kruczek, N.; Erickson, N.; France, K. Advanced environmentally resistant lithium fluoride mirror coatings for the next generation of broadband space observatories. *Appl. Opt.* **2017**, *56*, 9941–9950. [[CrossRef](#)]
29. Balasubramanian, K.; Hennessy, J.; Raouf, N.; Nikzad, S.; Ayala, M.; Shaklan, S.; Scowen, P.; Del Hoyo, J.; Quijada, M. Aluminum mirror coatings for UVOIR telescope optics including the far UV. *Proc. SPIE* **2015**, *9602*, 96020I. [[CrossRef](#)]
30. Hennessy, J.; Moore, C.S.; Balasubramanian, K.; Jewell, A.D.; France, F.; Nikzad, S. Enhanced atomic layer etching of native aluminum oxide for ultraviolet optical applications. *J. Vac. Sci. Technol. A* **2017**, *35*, 041512. [[CrossRef](#)]
31. Blakeney, K.J.; Winter, C.H. Atomic layer deposition of aluminum metal films using a thermally stable aluminum hydride reducing agent. *Chem. Mater.* **2018**, *30*, 1844–1848. [[CrossRef](#)]
32. Hausmann, D.M.; Gordon, R.G. Surface morphology and crystallinity control in the atomic layer deposition (ALD) of hafnium and zirconium oxide thin films. *J. Cryst. Growth* **2003**, *249*, 251–261. [[CrossRef](#)]

